

Measuring the Kerr spin parameter of a non-Kerr compact object with the continuum-fitting and the iron line methods

Cosimo Bambi

Center for Field Theory and Particle Physics & Department of Physics,
Fudan University, 200433 Shanghai, China

E-mail: bambi@fudan.edu.cn

Abstract. Under the assumption that astrophysical black hole candidates are the Kerr black holes of general relativity, the continuum-fitting method and the analysis of the $K\alpha$ iron line are today the only available techniques capable of providing a relatively reliable estimate of the spin parameter of these objects. If we relax the Kerr black hole hypothesis and we try to test the nature of black hole candidates, we find that there is a strong correlation between the measurement of the spin and possible deviations from the Kerr solution. The properties of the radiation emitted in a Kerr spacetime with spin parameter a_* are indeed very similar, and practically indistinguishable, from the ones of the radiation emitted around a non-Kerr object with different spin. In this paper, I address the question whether measuring the Kerr spin with both the continuum-fitting method and the $K\alpha$ iron line analysis of the same object can be used to claim the Kerr nature of the black hole candidate in the case of consistent results. In this work, I consider two non-Kerr metrics and it seems that the answer does depend on the specific background. The two techniques may either provide a very similar result (the case of the Bardeen metric) or show a discrepancy (Johannsen-Psaltis background).

Keywords: astrophysical black holes, modified gravity, X-rays.

Contents

1	Introduction	1
2	Continuum-fitting method	3
3	$K\alpha$ iron line	4
4	Testing the spacetime geometry around black hole candidates	5
5	Discussion	9
6	Summary and conclusions	11

1 Introduction

Today we have robust observational evidence for the existence of compact objects in X-ray binary systems with a mass $M \approx 5 - 20 M_{\odot}$, and of dark bodies at the center of every normal galaxy with $M \sim 10^5 - 10^9 M_{\odot}$ (for a review, see e.g. Ref. [1]). The masses of these objects are inferred by dynamical measurements, by studying the Newtonian orbital motion of gas or individual stars, and their estimate is thus reliable. It is thought that all these objects are the Kerr black holes (BHs) of general relativity. Stellar-mass BH candidates are indeed too heavy to be neutron or quark stars for any reasonable matter equation of state [2, 3]. The super-massive BH candidates at the centers of galaxies turn out to be too massive, compact, and old to be clusters of non-luminous objects, as the cluster lifetime due to evaporation and physical collisions would be shorter than the age of these systems [4]. The non-observation of thermal radiation emitted by the possible surface of BH candidates may also be interpreted as an indication for the existence of an event horizon [5, 6] (see however [7, 8]). But that is all we know. There is no direct evidence that BH candidates are Kerr BHs and current observations cannot rule out the possibility that the spacetime geometry around them significantly deviates from the Kerr solution [9, 10].

In 4-dimensional general relativity, uncharged BHs are described by the Kerr metric and they are completely specified by only two parameters: the mass M and the spin parameter $a_* = J/M^2$, where J is the BH spin angular momentum [11–13]. The condition for the existence of the event horizon is $|a_*| \leq 1$, while for $|a_*| > 1$ there is no BH and the central singularity is naked. All the properties of the spacetime can be immediately deduced from M and a_* . If astrophysical BH candidates are the Kerr BHs of general relativity, we just need to measure their mass and spin parameter to know everything about them. The mass M is relatively easy to obtain, as it can be inferred by studying the orbital motion of individual stars around the BH candidate in the framework of Newtonian mechanics; that is, without any assumption about the nature of the compact object. The measurement of the spin is much more challenging. The spin has indeed no gravitational effects in Newtonian mechanics and thus its measurement requires to probe the spacetime close to the compact object. That is possible, at least in principle, by studying the properties of the electromagnetic radiation emitted by the gas in the accretion disk.

At present, there are only two techniques capable of providing a relatively reliable measurement of the spin parameter of BH candidates under the assumption that the spacetime around them is described by the Kerr solution: the continuum-fitting method [14–16] and the analysis of the $K\alpha$ iron line [17, 18]. With the continuum-fitting method, one studies the thermal spectrum of geometrically thin and optically thick accretion disks and the spin parameter can be inferred from the position of the high energy cut-off. In the case of the iron line, one considers a line that is intrinsically narrow in frequency, while the one observed appears broadened and skewed due to special and general relativistic effects. Here the spin parameter is measured from the low energy tail of the line. Let us note that the continuum-fitting method can be applied only to stellar-mass BH candidates: the disk’s temperature scales as $M^{-0.25}$, so the high energy part of the spectrum is in the keV band for stellar-mass BH candidates and in the UV range for super-massive ones. In the latter case, dust absorption makes a measurement impossible. The iron line approach has not this problem, and it can be used to measure the spin of both stellar-mass and super-massive BH candidates.

Both the continuum-fitting method and the analysis of the $K\alpha$ iron line can be extended to non-Kerr backgrounds and be used to test the nature of BH candidates [19–27]. In this case, we cannot measure the spin parameter of the compact object, but only constrain a certain combination of the spin parameter and of possible deviations from the Kerr background. In other words, the thermal spectrum of thin disks and the shape of the $K\alpha$ iron line of Kerr BHs can be very similar, and practically indistinguishable, from the ones of a non-Kerr compact object with very different spin parameter.

How about we combine the two measurements? Can we break the degeneracy in the spin-deformation plane and get a measurement for both the spin and the deformations? In general, it is not easy to measure the spin of a stellar-mass BH candidate with both the continuum-fitting method and the iron line approach, as the former requires good observational data of the soft X-ray component, when the BH candidate is in the high-soft state, while the latter typically requires that the object is in the low-hard state. However, it is definitively possible in principle. The measurement of the spin parameter with both the techniques has been already done in Ref. [28] for the BH candidate XTE J1550-564, and it may become a routine analysis in the future, when more data will be available. To address this question, in this paper I study two different non-Kerr BH metrics: the Bardeen metric [29] and the Johannsen-Psaltis one [30]. While deformations of the Bardeen type seem to be more theoretically motivated, there may be theories with BHs similar to the Johannsen-Psaltis ones. The results of the present work show that the continuum-fitting and the iron line measurements, when combined and if consistent, cannot break this degeneracy in the Bardeen case, but they can potentially do it for Johannsen-Psaltis BHs. So, some caution should be in order before claiming that astrophysical BH candidates are the Kerr BHs of general relativity in the case in which the two approaches give very similar values of the Kerr spin, even for very accurate measurements.

The paper is organized as follows. In Sections 2 and 3, I briefly review, respectively, the continuum-fitting method and the $K\alpha$ iron line analysis. Section 4 is devoted to the use of these two techniques to test the nature of BH candidates and I compute their Kerr spin measurements in the case BH candidates are not Kerr BHs. In Section 5, I discuss these results. The conclusion is that the two approaches may be consistent even in the case of non-Kerr BHs, so some caution is definitively necessary. Summary and conclusions are reported in Section 6. Throughout the manuscript, I use units in which $G_N = c = 1$, unless stated otherwise.

2 Continuum-fitting method

Geometrically thin and optically thick accretion disks around BHs can be described by the Novikov-Thorne model [31]. In a generic stationary, axisymmetric, and asymptotically flat spacetime, one assumes that the disk is on the equatorial plane, that the disk's gas moves on nearly geodesic circular orbits, and that the energy is radiated from the disk's surface. From the conservation laws for the rest-mass, the angular momentum, and the energy, one obtains three basic equations for the time-averaged radial structure of the disk [32]. The time-averaged energy flux is given by

$$\mathcal{F}(r) = \frac{\dot{M}}{4\pi\sqrt{-G}}F(r), \quad (2.1)$$

where \dot{M} is the mass accretion rate, G is the determinant of the near equatorial plane metric in cylindrical coordinates, so $\sqrt{-G} = \sqrt{\alpha^2 g_{rr} g_{\phi\phi}}$ and α is the lapse function, and $F(r)$ is

$$F(r) = \frac{\partial_r \Omega}{(E - \Omega L_z)^2} \int_{r_{\text{in}}}^r (E - \Omega L_z)(\partial_\rho L_z) d\rho. \quad (2.2)$$

In Eq. (2.2), E , L_z , and Ω are, respectively, the conserved specific energy, the conserved z -component of the specific angular momentum, and the angular velocity for equatorial circular geodesics. r_{in} is the inner radius of the accretion disk and in the Novikov-Thorne model is assumed to be at the innermost stable circular orbit (ISCO).

Since the disk is in thermal equilibrium, the emission is blackbody-like and we can define an effective temperature $T_{\text{eff}}(r)$ from the relation $\mathcal{F}(r) = \sigma T_{\text{eff}}^4$, where σ is the Stefan-Boltzmann constant. Actually, the disk's temperature near the inner edge of the disk can be high, up to $\sim 10^7$ K for stellar-mass BH candidates, and non-thermal effects are non-negligible. That is usually taken into account by introducing the color factor (or hardening factor) f_{col} . The color temperature is $T_{\text{col}}(r) = f_{\text{col}} T_{\text{eff}}$ and the local specific intensity of the radiation emitted by the disk is

$$I_e(\nu_e) = \frac{2h\nu_e^3}{f_{\text{col}}^4} \frac{\Upsilon}{\exp\left(\frac{h\nu_e}{k_B T_{\text{col}}}\right) - 1}, \quad (2.3)$$

where ν_e is the photon frequency, h is the Planck's constant, k_B is the Boltzmann constant, and Υ is a function of the angle between the wavevector of the photon emitted by the disk and the normal of the disk surface, say ξ . The two most common options are $\Upsilon = 1$ (isotropic emission) and $\Upsilon = \frac{1}{2} + \frac{3}{4} \cos \xi$ (limb-darkened emission).

The calculation of the thermal spectrum of a thin accretion disk has been extensively discussed in the literature; see e.g. [15, 22] and references therein. The spectrum can be conveniently written in terms of the photon flux number density as measured by a distant observer, $N_{E_{\text{obs}}}$. In order to include all the relativistic effects, it is necessary to compute the photon trajectories from the disk, where the photon is emitted, to the image plane of the distant observer, where it is detected. The photon flux number density is eventually given by

$$\begin{aligned} N_{E_{\text{obs}}} &= \frac{1}{E_{\text{obs}}} \int I_{\text{obs}}(\nu) d\Omega_{\text{obs}} = \frac{1}{E_{\text{obs}}} \int w^3 I_e(\nu_e) d\Omega_{\text{obs}} = \\ &= A_1 \left(\frac{E_{\text{obs}}}{\text{keV}}\right)^2 \int \frac{1}{M^2} \frac{\Upsilon dX dY}{\exp\left[\frac{A_2}{wF^{1/4}} \left(\frac{E_{\text{obs}}}{\text{keV}}\right)\right] - 1}, \end{aligned} \quad (2.4)$$

where I_{obs} , E_{obs} , and ν are, respectively, the specific intensity of the radiation, the photon energy, and the photon frequency measured by the distant observer, X and Y are the coordinates of the position of the photon on the sky, as seen by the distant observer, and $d\Omega_{\text{obs}} = dXdY/D^2$, with D the distance of the source. w is the redshift factor

$$w = \frac{E_{\text{obs}}}{E_e} = \frac{\nu}{\nu_e} = \frac{k_\alpha u_{\text{obs}}^\alpha}{k_\beta u_e^\beta}, \quad (2.5)$$

$E_e = h\nu_e$, k^α is the 4-momentum of the photon, $u_{\text{obs}}^\alpha = (-1, 0, 0, 0)$ is the 4-velocity of the distant observer, and $u_e^\alpha = (u_e^t, 0, 0, \Omega u_e^t)$ is the 4-velocity of the emitter. $I_e(\nu_e)/\nu_e^3 = I_{\text{obs}}(\nu_{\text{obs}})/\nu^3$ follows from the Liouville's theorem. A_1 and A_2 are given by (here I show explicitly G_N and c)

$$A_1 = \frac{2(\text{keV})^2}{f_{\text{col}}^4} \left(\frac{G_N M}{c^3 h D} \right)^2 = \frac{0.07205}{f_{\text{col}}^4} \left(\frac{M}{M_\odot} \right)^2 \left(\frac{\text{kpc}}{D} \right)^2 \gamma \text{keV}^{-1} \text{cm}^{-2} \text{s}^{-1},$$

$$A_2 = \left(\frac{\text{keV}}{k_B f_{\text{col}}} \right) \left(\frac{G_N M}{c^3} \right)^{1/2} \left(\frac{4\pi\sigma}{\dot{M}} \right)^{1/4} = \frac{0.1331}{f_{\text{col}}} \left(\frac{10^{18} \text{g s}^{-1}}{\dot{M}} \right)^{1/4} \left(\frac{M}{M_\odot} \right)^{1/2}. \quad (2.6)$$

Using the normalization condition $g_{\mu\nu} u_e^\mu u_e^\nu = -1$, one finds

$$u_e^t = -\frac{1}{\sqrt{-g_{tt} - 2g_{t\phi}\Omega - g_{\phi\phi}\Omega^2}}, \quad (2.7)$$

and therefore

$$w = \frac{\sqrt{-g_{tt} - 2g_{t\phi}\Omega - g_{\phi\phi}\Omega^2}}{1 + \lambda\Omega}, \quad (2.8)$$

where $\lambda = k_\phi/k_t$ is a constant of the motion along the photon path. Doppler boosting, gravitational redshift, and frame dragging are entirely encoded in the redshift factor w .

3 $K\alpha$ iron line

The X-ray spectrum of both stellar-mass and supermassive BH candidates is usually characterized by the presence of a power-law component. This feature is commonly interpreted as the inverse Compton scattering of thermal photons by electrons in a hot corona above the accretion disk. The geometry of the corona is not known and several models have been proposed. Such a ‘‘primary component’’ irradiates also the accretion disk, producing a ‘‘reflection component’’ in the X-ray spectrum. The illumination of the cold disk by the primary component also produces spectral lines by fluorescence. The strongest line is the $K\alpha$ iron line at 6.4 keV. This line is intrinsically narrow in frequency, while the one observed appears broadened and skewed. Especially for some sources, this line is extraordinarily stable, in spite of a substantial variability of the continuum. This fact suggests that its shape is determined by the geometry of the spacetime around the compact object.

The profile of the $K\alpha$ iron line depends on the background metric, the geometry of the emitting region, the disk emissivity, and the disk's inclination angle with respect to the line of sight of the distant observer. In the Kerr spacetime, the only relevant parameter of the background geometry is the spin parameter a_* , while M sets the length of the system, without affecting the shape of the line. In those sources for which there is indication that

the line is mainly emitted close to the compact object, the emission region may be thought to range from the radius of the ISCO, $r_{\text{in}} = r_{\text{ISCO}}$, to some outer radius r_{out} . However, even more complicated geometries are possible. In principle, the disk emissivity could be theoretically calculated. In practice, that is not feasible at present. The simplest choice is an intensity profile $I_e \propto r^\alpha$ with index $\alpha < 0$ to be determined during the fitting procedure. The fourth parameter is the inclination of the disk with respect to the line of sight of the distant observer, i . The dependence of the line profile on a_* , i , α , and r_{out} in the Kerr background has been analyzed in detail by many authors, starting with Ref. [33]. The line profile in non-Kerr backgrounds is discussed in [24–27].

Roughly speaking, the calculation of the profile of the $K\alpha$ iron line goes as follows. We want to compute the photon flux number density measured by a distant observer, which is still given by

$$N_{E_{\text{obs}}} = \frac{1}{E_{\text{obs}}} \int I_{\text{obs}}(E_{\text{obs}}) d\Omega_{\text{obs}} = \frac{1}{E_{\text{obs}}} \int w^3 I_e(E_e) d\Omega_{\text{obs}}. \quad (3.1)$$

As the $K\alpha$ iron line is intrinsically narrow in frequency, we can assume that the disk emission is monochromatic (the rest frame energy is $E_{K\alpha} = 6.4$ keV) and isotropic with a power-law radial profile:

$$I_e(E_e) \propto \delta(E_e - E_{K\alpha}) r^\alpha. \quad (3.2)$$

The calculation of w is the same of the one for the disk’s thermal spectrum, as well as the calculation of the photon trajectories, from the point of emission in the disk to the image plane of the distant observer. More details can be found in Ref. [24].

4 Testing the spacetime geometry around black hole candidates

In both the continuum-fitting method and the analysis of the $K\alpha$ iron line, the background geometry sets the inner edge of the disk, which is supposed to be at the ISCO radius. That is a very important ingredient in the calculation of the properties of the radiation. In the disk’s spectrum, the inner edge of the disk determines the radiative efficiency of the accretion process, and thus the high energy cut-off of the spectrum, which is the key-point in the measurement of the spin. In the profile of the iron line, the inner edge of the disk determines the low energy tail of the line. The geometry of the spacetime enters also the calculations of the redshift factor w , of the propagation of the photons from the disk to the image plane of the observer, and of the time-averaged energy flux of the disk (for the thermal spectrum of the disk). If we want to test the Kerr nature of an astrophysical BH candidate, it is convenient to consider a general spacetime in which the central object is described by a mass M , spin parameter a_* , and one (or more) “deformation parameter(s)”. The latter measure possible deviations from the Kerr solution, which must be recovered when all the deformation parameters vanish. The strategy is thus to calculate the properties of the radiation emitted by the gas in the accretion disk in these more general backgrounds and then fit the observational data of the source to find the allowed values of the spin and of the deformation parameters. If the observations require vanishing deformation parameters, the compact object is a Kerr BH. If they demand non-vanishing deformation parameters, astrophysical BH candidates are not the Kerr BH of general relativity and new physics is necessary. In general, however, the result is that observations allows both the possibility of a Kerr BH with a certain spin parameter and non-Kerr objects with different spin parameters.

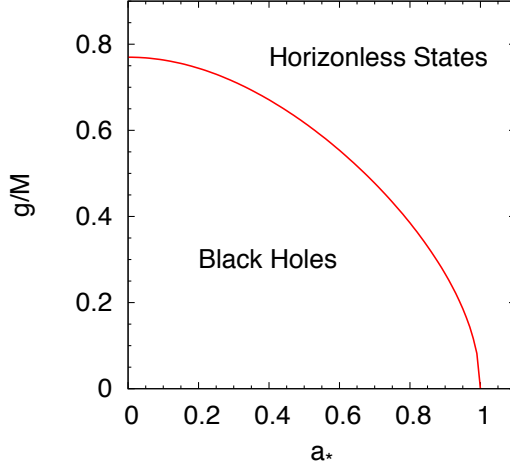


Figure 1. Rotating Bardeen metric. The red solid line separates the region with BHs from the one with horizonless objects.

As test-metric, let us consider the rotating Bardeen black hole solution [29]:

$$\begin{aligned}
 ds^2 = & - \left(1 - \frac{2mr}{\Sigma} \right) dt^2 - \frac{4amr \sin^2 \theta}{\Sigma} dt d\phi + \frac{\Sigma}{\Delta} dr^2 + \Sigma d\theta^2 + \\
 & + \sin^2 \theta \left(r^2 + a^2 + \frac{2a^2mr \sin^2 \theta}{\Sigma} \right) d\phi^2,
 \end{aligned} \tag{4.1}$$

where $a = J/M$, $\Sigma = r^2 + a^2 \cos^2 \theta$, $\Delta = r^2 - 2mr + a^2$, and

$$m = \frac{Mr^3}{(r^2 + g^2)^{3/2}}. \tag{4.2}$$

The deformation parameter is the charge g and the Kerr metric is recovered when $g = 0$. The radius of the event horizon is given by the larger root of $\Delta = 0$. If the equation $\Delta = 0$ has no solutions, the object is not a BH but a configuration without horizon. The regions of BHs and horizonless states on the plane $(a_*, g/M)$ are shown in Fig. 1. In what follows, I will restrict the attention to the BH region: even if they can be created [35], the horizonless states are likely very unstable objects with a short lifetime due to the ergoregion instability.

Let us now consider the possibility that an astrophysical BH candidate is a Bardeen BH and that we want to measure the spin parameter of this object with the continuum-fitting method and the $K\alpha$ iron line analysis, assuming that the object is a Kerr BH. In this case, we can use an approach similar to the one discussed in Ref. [24] and define the reduced χ^2 , respectively for the disk's thermal spectrum and the iron line profile:

$$\chi_{\text{disk, red}}^2(a_*^{\text{Kerr}}, i) = \frac{1}{n} \sum_{i=1}^n \frac{[N_{\text{disk } i}^{\text{Kerr}}(a_*^{\text{Kerr}}, i) - N_{\text{disk } i}^{\text{B}}(a_*^{\text{B}}, g/M, i^{\text{B}})]^2}{\sigma_i^2}, \tag{4.3}$$

$$\chi_{\text{iron, red}}^2(a_*^{\text{Kerr}}, i) = \frac{1}{n} \sum_{i=1}^n \frac{[N_{\text{iron } i}^{\text{Kerr}}(a_*^{\text{Kerr}}, i) - N_{\text{iron } i}^{\text{B}}(a_*^{\text{B}}, g/M, i^{\text{B}})]^2}{\sigma_i^2}, \tag{4.4}$$

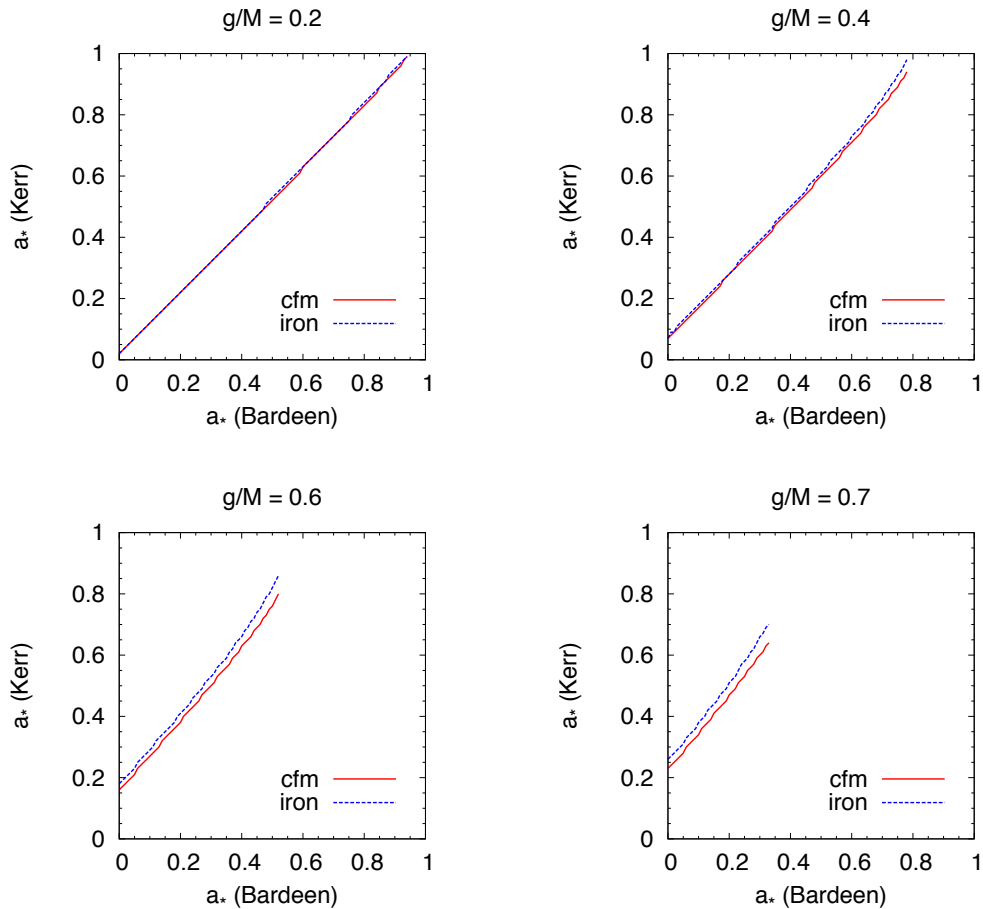


Figure 2. Kerr spin measurement via the continuum-fitting method (red solid lines) and the iron line analysis (blue dashed lines) in the case the astrophysical source is a rotating Bardeen black hole with $g/M = 0.2$ (top left panel), 0.4 (top right panel), 0.6 (bottom left panel), and 0.7 (bottom right panel). Even if for high values of g/M the difference between the actual value of the spin parameter and the one inferred assuming the Kerr background can be significant, the two techniques provide quite similar estimates. See the text for details.

where the summation is performed over n sampling energies E_i and N_i^{Kerr} and N_i^{B} are the photon fluxes (normalized photon fluxes in the case of the iron line profile) in the energy bin $[E_i, E_i + \Delta E]$, respectively for the Kerr and the Bardeen metric. The error σ_i is assumed to be 15% the photon flux N_i^{B} , which is roughly the accuracy of current observations in the best situations. For the analysis, I take $i^{\text{B}} = 45^\circ$ and $43^\circ < i < 47^\circ$, assuming that the inclination angle of the disk is known from independent observations with an accuracy $\pm 2^\circ$. However, the final result is not sensitive to the exact choices of i^{B} and Δi . For the disk's spectrum, all the calculations are done with $M = 10 M_\odot$ and $\dot{M} = 2 \cdot 10^{18} \text{ g s}^{-1}$. The mass accretion rate should actually be inferred during the fitting procedure, but here we can assume to be known as its determination is independent of the spin measurement. In the case of the iron line, all the calculations are done with an intensity profile index $\alpha = -3$ and an outer radius $r_{\text{out}} = r_{\text{in}} + 100 M$.

At this point, one can consider a specific value of a_*^{B} and g/M and find the minimum

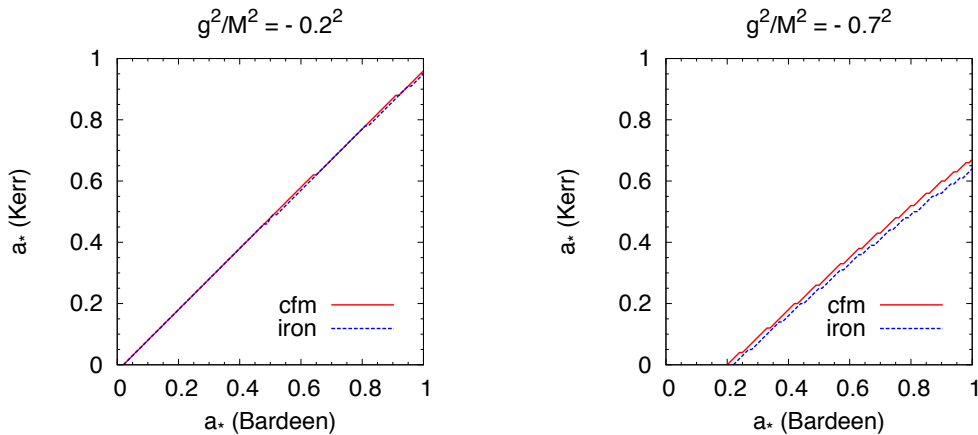


Figure 3. As in Fig. 2, for $g^2/M^2 = -0.2^2$ (left panel) and -0.7^2 (right panel). See the text for details.

of the reduced χ^2 , thus obtaining the measurement of the Kerr spin parameter. The results are reported in Fig. 2 for $g/M = 0.2$ (left top panel), 0.4 (right top panel), 0.6 (left bottom panel), and 0.7 (right bottom panel), respectively for the disk's thermal spectrum (red solid lines) and the iron line (blue dashed lines). Let us note a few important things. First, in all these cases the fit with the Kerr metric is good, in the sense that the minimum of χ_{red}^2 is $\ll 1$, for both the continuum-fitting method and the $K\alpha$ iron line analysis. So, the properties of these spectra are really indistinguishable from the one of a disk around a Kerr BH. Second, the two techniques provide quite similar results. For $g/M = 0.2$, the discrepancy is always $\Delta a_*^{\text{Kerr}} \lesssim 0.01$. For $g/M = 0.7$, the difference between the spin measurements of the two approaches ranges from $\Delta a_*^{\text{Kerr}} \approx 0.03$, for non-rotating and slow-rotating Bardeen BHs, to $\Delta a_*^{\text{Kerr}} \approx 0.06$, for near extremal objects. The spin range is $a_*^{\text{B}} < 0.95$ for $g/M = 0.2$, $a_*^{\text{B}} < 0.79$ for $g/M = 0.4$, $a_*^{\text{B}} < 0.53$ for $g/M = 0.6$, and $a_*^{\text{B}} < 0.34$ for $g/M = 0.7$ because for higher spins there are no BHs, but some kind of horizonless states (like the Kerr metric with $a_*^{\text{Kerr}} > 1$, but without central singularity). Because of the ergoregion instability, fast-rotating compact objects without an event horizon are expected to be very unstable, and so not good BH candidates. However, even if they were stable, their features would be very different and thus these objects would be easy to distinguish from Kerr BHs.

Fig. 2 shows that the inferred Kerr spin parameter is always higher than its actual value. This is only the consequence of the specific form of the Bardeen metric, in which the gravitational force is weaker than the one around a Kerr BH with the same spin. To have a stronger gravitational field, we just need that g^2 in Eq. (4.2) is negative. While such a possibility is against the original motivation of the Bardeen metric, i.e. to have a singularity free BH solution, we can surely consider this case in our approach. When $g^2 < 0$, the measurement of the Kerr spin provides a value lower than the actual spin parameter of the object, as shown in Fig. 3. However, the difference between the results obtained via the continuum-fitting and the iron line methods are still quite similar.

5 Discussion

The thermal spectrum of a geometrically thin disk is determined by the mass of the compact object, its distance from us, the inclination angle of the disk with respect to the observer's line of sight, the mass accretion rate, and the spin (assuming the Kerr background; otherwise the spin and the deformation parameter(s) if we want to test the nature of the BH candidate). The first three parameters (mass, distance, viewing angle) must be known from independent measurements. One can then fit the soft X-ray component of the spectrum of the source and obtain the mass accretion rate and the background parameters. It is clear that the source must be in the high-soft state, when the component from the disk is dominant. In the case of the iron line analysis, the mass and the distance of the compact object do not enter the calculations of the line profile, while the viewing angle can be inferred during the fitting procedure and it is thus not an input parameter. Good data of the iron line usually require that the source is in the low-hard state. From this considerations, it follows that it is not obvious to be able to measure the spin parameter with both the continuum-fitting method and the $K\alpha$ iron analysis of the same source, as we need different conditions and observations.

In Ref. [28], the authors consider the BH candidate in XTE J1550-564 and they measure the Kerr spin parameter of this object with the analysis of the disk's thermal spectrum and of the iron line profile. They find

$$a_*^{\text{Kerr}} = 0.34_{-0.28}^{+0.23} \text{ (68\% C.L.)}, \quad 0.34_{-0.45}^{+0.37} \text{ (90\% C.L.)} \quad (\text{disk's spectrum}), \quad (5.1)$$

$$a_*^{\text{Kerr}} = 0.55_{-0.11}^{+0.05} \text{ (68\% C.L.)}, \quad 0.55_{-0.22}^{+0.15} \text{ (90\% C.L.)} \quad (\text{iron line}). \quad (5.2)$$

The two measurement are consistent, but the uncertainty is quite large. From the results of the previous section, it is clear that to distinguish a Kerr BH from a Bardeen one with the measurement of the Kerr spin we need, in the most optimistic situation of a fast-rotating object with large g/M , measurements with an accuracy at the level of $\Delta a_*^{\text{Kerr}} \approx 0.02$, much better than what we can do now and presumably out of reach even in the future.

Are we really so far from being able to test the Kerr nature of BH candidates? Actually, if we consider a different test-metric, our chances may not be so bad. To be more specific, let us replace the rotating Bardeen solution with the Johannsen-Psaltis (JP) metric, proposed in Ref. [30] explicitly to be used as a metric to test the Kerr BH hypothesis and potentially capable of describing non-Kerr BHs in a putative alternative theory of gravity. In its simplest version, the line element in Boyer-Lindquist coordinates reads

$$ds^2 = - \left(1 - \frac{2Mr}{\Sigma} \right) (1+h) dt^2 - \frac{4aMr \sin^2 \theta}{\Sigma} (1+h) dt d\phi + \frac{\Sigma (1+h)}{\Delta + a^2 h \sin^2 \theta} dr^2 + \Sigma d\theta^2 + \left[\left(r^2 + a^2 + \frac{2a^2 Mr \sin^2 \theta}{\Sigma} \right) \sin^2 \theta + \frac{a^2 (\Sigma + 2Mr) \sin^4 \theta}{\Sigma} h \right] d\phi^2, \quad (5.3)$$

where now $\Delta = r^2 - 2Mr + a^2$ and

$$h = \frac{\epsilon_3 M^3 r}{\Sigma^2}. \quad (5.4)$$

Here ϵ_3 is the deformation parameter. The compact object is more prolate (oblate) than a Kerr BH for $\epsilon_3 > 0$ ($\epsilon_3 < 0$); when $\epsilon_3 = 0$, we recover the Kerr solution.

If we proceed as in the previous section and we compare the Kerr spin measurements via the continuum-fitting and the iron line methods, we find that the discrepancy between

the two techniques may be larger. In Fig. 4, I show the cases $\epsilon_3 = -2, 2, 4,$ and 8 . Here it is not really clear the maximum value of the spin parameter that makes sense to consider. In Fig. 4, I considered spins from 0 to 1. The end of the lines in the left panel of Fig. 4 is simply due that for higher values of the spin parameter the fits become bad and the minimum of χ_{red}^2 exceeds 1. So, at this point the two metrics (JP and Kerr) become very different and even a single measurement (continuum-fitting or iron line) can check if the BH candidate is or is not a Kerr BH. However, these cases with a bad fit are usually configurations with naked singularities, whose physical meaning would be anyway questionable. In the case $\epsilon_3 = 8$, the discrepancy between the Kerr spin measurements of the two techniques is $\Delta a_*^{\text{Kerr}} \approx 0.25$, quite independently of the exact value of the spin for slow-rotating and mid-rotating objects. While these results may suggest that future X-ray data could really test the nature of a BH candidate, it is important to stress a fundamental difference between the metric in Eq. (4.1) and the one in (5.3). The Bardeen metric is an acceptable BH solution in presence of exotic matter and presumably even in the case of extensions of general relativity. The JP metric is obtained with an arbitrary procedure and it is definitively not clear if such kinds of deformations from the Kerr geometry can be obtained from a consistent theory. It is found by starting from a deformed Schwarzschild solution and it is transformed into a rotating solution with the Newman-Janis algorithm. However, the initial deformed non-rotating metric has $g_{tt} \neq -1/g_{rr}$, which is not the case one would expect for a BH. More importantly, the transformation to get the metric in Boyer-Lindquist coordinates is not a valid coordinate transformation [29] (see also the discussion in Ref. [34]). The result is that the metric has some quite pathological features [36]. So, the interpretation of these results remain ambiguous, but at least they show that a discrepancy between the continuum-fitting method and the iron line analysis is not necessarily tiny and it depends on the specific background metric.

Finally, one can also consider the possibility of using other approaches to combine with the measurements of the disk’s spectrum or of the iron line profile. Unfortunately, however, other methods are not yet mature to probe the spacetime geometry around BH candidates [1]. The estimate of the radiative efficiency has been applied to non-Kerr backgrounds in Refs. [37–39], but it can only provide a quite rough estimate of possible deviations from the Kerr solution. Quasi-periodic oscillations seen in the X-ray spectrum of stellar-mass BH candidates may potentially be a quite powerful tool, but at present the exact mechanism responsible for these features is not known and different models provide different results [40]. An accurate observation of the boundary of the “shadow” of BH candidates is also a very interesting possibility, but it requires the use of sub-mm wavelength and the necessary precision to test the Kerr metric may be out of reach for the near future [41–45]. Recently, there has been some interest in the possibility of measuring the spin parameter (or both the spin and the deformation parameters) from the estimate of the jet power [46–49]. The basic idea is that, if some kind of jets are powered by the spin of the compact object, the power of the jet should be correlated to the value of the spin parameter. Such an approach to measure the spin of the compact object should be really independent of the background geometry and therefore its combination with either the continuum-fitting measurement or the iron line one would have the capability of revealing a possible non-Kerr nature of the BH candidate, at least for large deformations, as shown in Fig. 5 for the Bardeen metric with $g/M = 0.2$ and 0.7 . The issue is however quite controversial [50, 51], and, depending if one assumes that steady or transient jets are powered by the BH spin, current data would suggest different conclusions [48, 49].

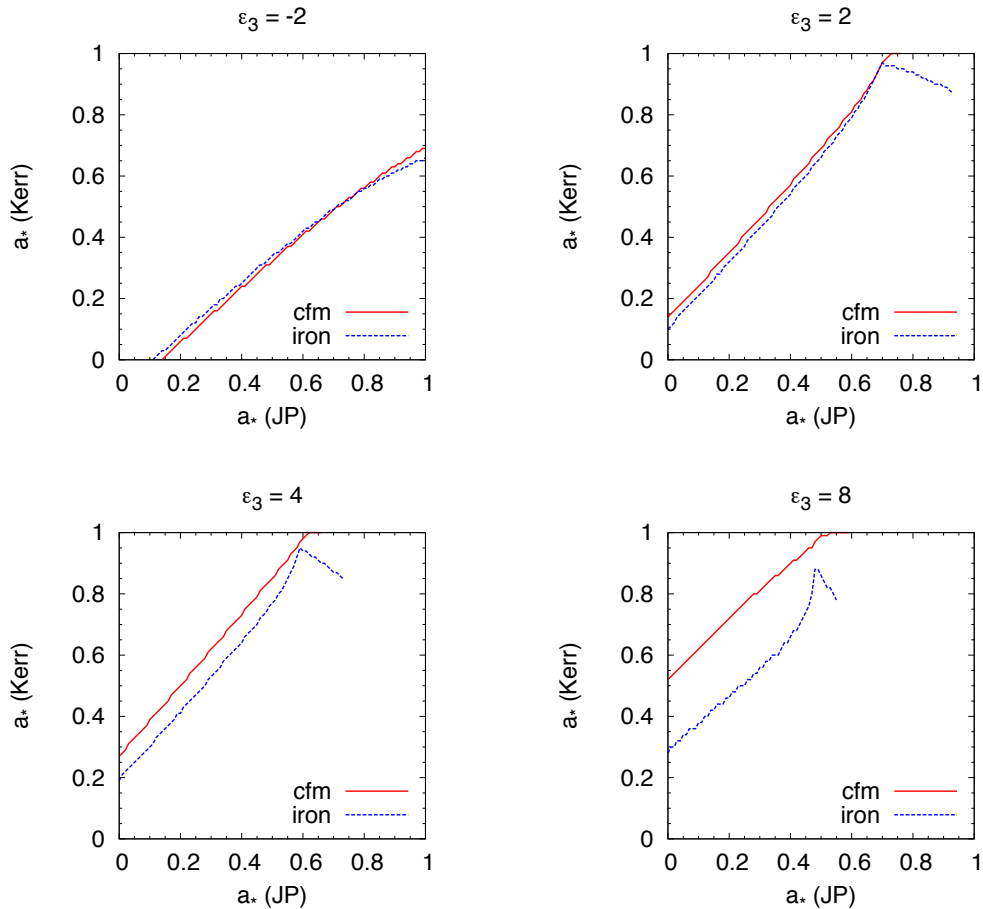


Figure 4. As in Fig. 2, for the JP metric with $\epsilon_3 = -2$ (top left panel), 2 (top right panel), 4 (bottom left panel), and 8 (bottom right panel). See the text for details.

6 Summary and conclusions

Astrophysical BH candidates are stellar-mass compact objects in X-ray binary systems and super-massive dark bodies at the center of every normal galaxy. They are thought to be the Kerr BH of general relativity, but the actual nature of these objects has still to be verified. To test the Kerr BH hypothesis, we have to probe the spacetime geometry around these compact objects and check if there are deviations from the predictions of general relativity. This can be achieved by studying the properties of the radiation emitted by the gas in the accretion disk. Today we have only two relatively robust techniques to probe the spacetime geometry around astrophysical BH candidates: the continuum-fitting method and the analysis of the relativistic iron line profile. If we assume that these objects are Kerr BHs, both the techniques can provide an estimate of the spin parameter. If we relax the Kerr assumption and we try to test the nature of the compact object, it turns out that we can only constrain a certain combination of the spin and of possible deviations from the Kerr solution. In other words, both the disk's thermal spectrum and the iron line profile of a Kerr BH with spin parameter a_* is very similar, and practically indistinguishable, from the ones of non-Kerr objects with different spin parameters. In particular, observations allow larger and larger deviations from

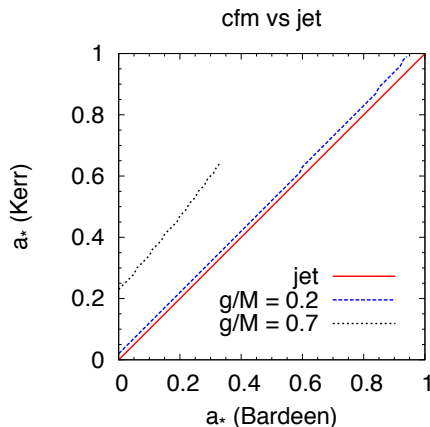


Figure 5. Comparison of the Kerr spin measurements via the jet power and the continuum-fitting method in the case the astrophysical source is a rotating Bardeen BH. The jet power approach may really measure the spin parameter of the object, independently of its actual nature. See the text for details.

the Kerr metric for more and more different spins with respect to the one expected from a Kerr BH.

In this paper, I have discussed the quite natural question whether the use of the two techniques for a specific object can break the strong correlation between the spin and the deformations. Astronomers may indeed be particularly interested to know if consistent measurements of the Kerr spin with the continuum-fitting method and the iron line analysis can be used to claim the Kerr nature of the BH candidate. The result of the present work is that the answer is not necessarily positive: at least in some non-Kerr metrics, the continuum-fitting method and the analysis of the iron line profile may provide very similar results and it is eventually impossible to distinguish a Kerr BH from another object. So, we should be careful about a possible degeneracy between the spin and deviations from the Kerr background. The reason of this degeneracy is only partially due to the common assumption of the two techniques that the inner edge of the disk is at the ISCO radius. Indeed, the combination of the two methods may fix this problem in other backgrounds (the JP metric is at least an example, even if its physical meaning is less clear). The main reason seems instead to come from the form of the Bardeen metric, which, however, is quite natural from a theoretical point of view [29]: such a metric can be written in Boyer-Lindquist coordinates as the Kerr one with the mass M replaced by a mass function $m(r)$, going to M at large radii. Other approaches, like the estimate of the jet power, are interesting possibilities to be combine with the continuum-fitting method and the $K\alpha$ iron line analysis to test even this kind of metrics.

Acknowledgments

This work was supported by the Thousand Young Talents Program and Fudan University.

References

- [1] R. Narayan, *New J. Phys.* **7**, 199 (2005) [gr-qc/0506078].

- [2] C. E. Rhoades and R. Ruffini, *Phys. Rev. Lett.* **32**, 324 (1974).
- [3] V. Kalogera and G. Baym, *Astrophys. J.* **470**, L61 (1996).
- [4] E. Maoz, *Astrophys. J.* **494**, L181 (1998) [astro-ph/9710309].
- [5] R. Narayan and J. E. McClintock, *New Astron. Rev.* **51**, 733 (2008) [arXiv:0803.0322 [astro-ph]].
- [6] A. E. Broderick, A. Loeb and R. Narayan, *Astrophys. J.* **701**, 1357 (2009) [arXiv:0903.1105 [astro-ph.HE]].
- [7] M. A. Abramowicz, W. Kluzniak and J. -P. Lasota, *Astron. Astrophys.* **396**, L31 (2002) [astro-ph/0207270].
- [8] C. Bambi, arXiv:1205.4640 [gr-qc].
- [9] C. Bambi, *Mod. Phys. Lett. A* **26**, 2453 (2011) [arXiv:1109.4256 [gr-qc]].
- [10] C. Bambi, *Astron. Rev.* **8**, 4 (2013) [arXiv:1301.0361 [gr-qc]].
- [11] B. Carter, *Phys. Rev. Lett.* **26**, 331 (1971).
- [12] D. C. Robinson, *Phys. Rev. Lett.* **34**, 905 (1975).
- [13] P. T. Chrusciel, J. L. Costa and M. Heusler, *Living Rev. Rel.* **15**, 7 (2012) [arXiv:1205.6112 [gr-qc]].
- [14] S. N. Zhang, W. Cui and W. Chen, *Astrophys. J.* **482**, L155 (1997) [astro-ph/9704072].
- [15] L. -X. Li, E. R. Zimmerman, R. Narayan and J. E. McClintock, *Astrophys. J. Suppl.* **157**, 335 (2005) [astro-ph/0411583].
- [16] J. E. McClintock, R. Narayan, S. W. Davis, L. Gou, A. Kulkarni, J. A. Orosz, R. F. Penna and R. A. Remillard *et al.*, *Class. Quant. Grav.* **28**, 114009 (2011) [arXiv:1101.0811 [astro-ph.HE]].
- [17] A. C. Fabian, K. Iwasawa, C. S. Reynolds and A. J. Young, *Publ. Astron. Soc. Pac.* **112**, 1145 (2000) [astro-ph/0004366].
- [18] C. S. Reynolds and M. A. Nowak, *Phys. Rept.* **377**, 389 (2003) [astro-ph/0212065].
- [19] T. Harko, Z. Kovacs and F. S. N. Lobo, *Phys. Rev. D* **78**, 084005 (2008) [arXiv:0808.3306 [gr-qc]].
- [20] T. Harko, Z. Kovacs and F. S. N. Lobo, *Phys. Rev. D* **80**, 044021 (2009) [arXiv:0907.1449 [gr-qc]].
- [21] T. Harko, Z. Kovacs and F. S. N. Lobo, *Class. Quant. Grav.* **27**, 105010 (2010) [arXiv:0909.1267 [gr-qc]].
- [22] C. Bambi and E. Barausse, *Astrophys. J.* **731**, 121 (2011) [arXiv:1012.2007 [gr-qc]].
- [23] C. Bambi, *Astrophys. J.* **761**, 174 (2012) [arXiv:1210.5679 [gr-qc]].
- [24] C. Bambi, *Phys. Rev. D* **87**, 023007 (2013) [arXiv:1211.2513 [gr-qc]].
- [25] C. Bambi, *Phys. Rev. D* **87**, 084039 (2013) [arXiv:1303.0624 [gr-qc]].
- [26] T. Johannsen and D. Psaltis, arXiv:1202.6069 [astro-ph.HE].
- [27] C. Bambi and D. Malafarina, arXiv:1307.2106 [gr-qc];
- [28] J. F. Steiner, R. C. Reis, J. E. McClintock, R. Narayan, R. A. Remillard, J. A. Orosz, L. Gou and A. C. Fabian *et al.*, *Mon. Not. Roy. Astron. Soc.* **416**, 941 (2011) [arXiv:1010.1013 [astro-ph.HE]].
- [29] C. Bambi and L. Modesto, *Phys. Lett. B* **721**, 329 (2013) [arXiv:1302.6075 [gr-qc]].
- [30] T. Johannsen and D. Psaltis, *Phys. Rev. D* **83**, 124015 (2011) [arXiv:1105.3191 [gr-qc]].

- [31] I. D. Novikov, K. S. Thorne, “Astrophysics of Black Holes” in *Black Holes*, edited by C. De Witt and B. De Witt (Gordon and Breach, New York, New York, 1973), pp. 343-450.
- [32] D. N. Page and K. S. Thorne, *Astrophys. J.* **191**, 499 (1974).
- [33] A. C. Fabian, M. J. Rees, L. Stella and N. E. White, *Mon. Not. Roy. Astron. Soc.* **238**, 729 (1989).
- [34] M. Azreg-Ainou, *Class. Quant. Grav.* **28**, 148001 (2011) [arXiv:1106.0970 [gr-qc]].
- [35] Z. Li and C. Bambi, *Phys. Rev. D* **87**, 124022 (2013) [arXiv:1304.6592 [gr-qc]].
- [36] C. Bambi and L. Modesto, *Phys. Lett. B* **706**, 13 (2011) [arXiv:1107.4337 [gr-qc]].
- [37] C. Bambi, *Phys. Rev. D* **83**, 103003 (2011) [arXiv:1102.0616 [gr-qc]].
- [38] C. Bambi, *Phys. Lett. B* **705**, 5 (2011) [arXiv:1110.0687 [gr-qc]].
- [39] C. Bambi, *Phys. Rev. D* **85**, 043001 (2012) [arXiv:1112.4663 [gr-qc]].
- [40] C. Bambi, *JCAP* **1209**, 014 (2012) [arXiv:1205.6348 [gr-qc]].
- [41] C. Bambi and K. Freese, *Phys. Rev. D* **79**, 043002 (2009) [arXiv:0812.1328 [astro-ph]].
- [42] C. Bambi and N. Yoshida, *Class. Quant. Grav.* **27**, 205006 (2010) [arXiv:1004.3149 [gr-qc]].
- [43] T. Johannsen and D. Psaltis, *Astrophys. J.* **718**, 446 (2010) [arXiv:1005.1931 [astro-ph.HE]].
- [44] C. Bambi, F. Caravelli and L. Modesto, *Phys. Lett. B* **711**, 10 (2012) [arXiv:1110.2768 [gr-qc]].
- [45] C. Bambi, *Phys. Rev. D* **87**, 107501 (2013) [arXiv:1304.5691 [gr-qc]].
- [46] R. Narayan and J. E. McClintock, *Mon. Not. Roy. Astron. Soc.* **419**, L69 (2012) [arXiv:1112.0569 [astro-ph.HE]].
- [47] J. F. Steiner, J. E. McClintock and R. Narayan, *Astrophys. J.* **762**, 104 (2013) [arXiv:1211.5379 [astro-ph.HE]].
- [48] C. Bambi, *Phys. Rev. D* **85**, 043002 (2012) [arXiv:1201.1638 [gr-qc]].
- [49] C. Bambi, *Phys. Rev. D* **86**, 123013 (2012) [arXiv:1204.6395 [gr-qc]].
- [50] R. Fender, E. Gallo and D. Russell, *Mon. Not. Roy. Astron. Soc.* **406**, 1425 (2010) [arXiv:1003.5516 [astro-ph.HE]].
- [51] D. M. Russell, E. Gallo and R. P. Fender, *Mon. Not. Roy. Astron. Soc.* **431**, 405 (2013) [arXiv:1301.6771 [astro-ph.HE]].